# Testing microscopic medium effects on nucleons and mesons using polarization observables in high-spin, unnatural-parity $(\vec{p},\vec{p}')$ reactions at 200 MeV

F. Sammarruca
*University of Idaho, Moscow, Idaho 83843*

E. J. Stephenson, K. Jiang,* J. Liu,† C. Olmer, A. K. Opper,‡ and S. W. Wissink
*Indiana University Cyclotron Facility, Bloomington, Indiana 47408*

(Received 13 May 1999; published 20 December 1999)

We compare measurements of the cross section, analyzing power, induced polarization, and polarization transfer coefficients for $(\vec{p},\vec{p}')$ reactions leading to unnatural-parity, high-spin states in $^{16}$O and $^{28}$Si with distorted wave impulse approximation calculations. We use an effective nucleon-nucleon (*NN*) interaction obtained from a microscopic treatment of nuclear medium effects. The *NN* potential is generated from a one-boson-exchange model of the nuclear force that reproduces *NN* scattering data well. Medium effects are incorporated through a *G* matrix obtained within a Dirac-Brueckner approach to nuclear matter. While agreement for some observables is good, differences for the polarization transfer coefficients indicate that systematic problems with the relative sizes of the spin-orbit and tensor interaction components exist. The differences are larger for $^{28}$Si than for $^{16}$O. A new model that incorporates density-dependent meson mass reductions produces only small effects that do not change the quality of the agreement. Connections to previous calculations are investigated.

PACS number(s): 21.30.Fe, 25.40.Ep, 24.10.Cn, 24.70.+s

## I. INTRODUCTION

Proton-nucleus inelastic scattering offers one of the simplest and cleanest ways to test whether models that incorporate medium modifications into an effective nucleon-nucleon (*NN*) force are adequate to describe nuclear reactions. In particular, the polarization observables are essentially determined by the spin dependence of the *NN* interaction [1,2] and provide an excellent way to check the spin-dependent *NN* amplitudes.

To facilitate the handling of this complicated many-body problem, the effects of the surrounding nucleons are incorporated into an effective *NN* interaction where differences from the original free *NN* force increase with nuclear density. Experiments completed over the past few years near 200 MeV now offer high precision polarization data for a number of discrete nuclear states. These data can be used to test models of the effective *NN* interaction below the pion production threshold where the free *NN* interaction is well constrained by the available two-body data.

In a previous paper, we described a microscopic treatment of the in-medium effective interaction [3]. The *NN* force was obtained from a one-boson-exchange (OBE) potential whose parameters had been adjusted to reproduce well the results of modern phase shift analyses below 350 MeV [4]. Comparisons to *NN* data measured near 200 MeV show excellent agreement. The systematic effects of placing this *NN* force within the nuclear medium are calculated using a *G*-matrix approach for infinite nuclear matter that incorporates nuclear binding and Pauli blocking effects [5]. This approach can also include the strong mean field scalar and vector potentials that are part of a covariant treatment of nucleon motion within nuclear matter [6–9]. We will refer to all of these mechanisms as ''conventional'' medium effects.

Distorted wave impulse approximation (DWIA) calculations based on this effective *NN* interaction model were compared to a body of $(p,p')$ cross section and analyzing power data for largely collective natural-parity transitions [3]. Previous work has shown that for such cases, a good description of the analyzing power implies that the polarization transfer coefficients will also be well reproduced [10]. We find that our model provides a satisfactory description of inelastic scattering to natural-parity states.

Natural-parity transitions are primarily sensitive to the isoscalar spin-independent and spin-orbit components of the interaction. For the investigation of other components, the main purpose of this paper, different transitions are needed. The high-spin stretched transitions offer a particularly good choice. Their unnatural parity makes them sensitive to the spin-orbit and all of the tensor components in the effective interaction. Because of their high spin, there is usually only one particle-hole configuration that contributes significantly to the transition, and the pertinent wavefunctions are easily constrained by transverse $(e,e')$ form factor measurements. Furthermore, these transitions are among the largest in the $(p,p')$ excited state spectrum and appropriate for studies using single-step Born approximation reaction calculations. Lower spin unnatural-parity states are also sensitive to the same components of the effective interaction, but pick up sensitivities to nuclear currents and finite-range exchange that complicate the analysis [11]. In addition, the polarization observables for the lower spin states are sensitive to how the amplitudes for the many possible particle-hole structure contributions are chosen, and other data is usually of scant help in making the right choice.

*Present address: MCI WorldCom, Oakbrook Terrace, IL 60181.
†Present address: Shell Oil Corporation, Houston, TX 77025.
‡Present address: Ohio University, Athens, OH 45701.

 

For this study we will consider the three $4^-$ states at 17.78, 18.98, and 19.81 MeV in $^{16}$O, as well as the two $6^-$ states at 11.58 and 14.35 MeV in $^{28}$Si. States of both $T=0$ and $T=1$ isospin character are present, giving us access to both isoscalar and isovector parts of the effective *NN* interaction. These measurements, made for proton energies near 200 MeV, have been reported on a number of prior occasions [12–15]. The experiments on $^{28}$Si are now completed [16], and all polarization transfer coefficients are available for comparison.

DWIA calculations reproduce the main trends of these measurements, as will be discussed in Sec. II. But several notable differences exist, especially for the diagonal polarization transfer coefficients. The nature of the discrepancies leads us to conclude that there are physical mechanisms missing from our model, despite efforts to constrain it through independent empirical information.

Our presentation of results will also include (Sec. II C) a comparison with combinations of polarization transfer coefficients expressed as polarized cross sections. Because of their selective dependence upon individual spin-dependent *NN* amplitudes in a Kerman, MaManus, and Thaler (KMT) [17] or Bystricky [18] representation, these polarized cross sections can be used as a powerful diagnostic tool.

At the end of Sec. II, we check the assumption that the isospin of these transitions is well known. We find no evidence that isospin mixing would offer an appropriate solution to the problems we encounter with these data.

Having observed that the established medium effects contained in our model do not provide an adequate description of these states, in Secs. III and IV we explore less conventional mechanisms. Because these data support the need for a substantial reduction of the tensor attraction in the medium, particular attention will be paid to those contributions which can affect the tensor force.

One way to reduce the tensor attraction is to increase the repulsive influence of the $\rho$ meson by systematically reducing its mass with increasing nuclear density. Known as Brown-Rho scaling [19,20], this mechanism would signal a change of the system toward a partial restoration of chiral symmetry. The suggestion is supported by QCD sum rule calculations that predict a mass reduction of about 20% at full nuclear matter density [21–24].

From the experimental side, evidence for in-medium $\rho$-meson mass reductions has been reported from diverse places, including proton elastic and inelastic scattering [25,26], measurements of polarization transfer in $(p,p')$ reactions [12,13,27], dilepton production in relativistic heavy ion collisions [28,29], and $\rho$-meson photoproduction and decay [30,31]. In some cases more conventional explanations have been offered [32,33], so the interpretation of these experiments remains an open question. In Sec. III, we will evaluate the impact of $\rho$-meson mass scaling on $(p,p')$ inelastic scattering within the context of a full density-dependent calculation.

While searching for improvements in the quality of $(p,p')$ predictions, it is desirable to keep as a constraint a realistic description of nuclear matter saturation properties, not an easy task in the presence of uniform meson mass scaling [34]. Recently, a model has been proposed [35] which combines Brown-Rho scaling together with a microscopic description of the intermediate-range attraction in terms of a correlated pair of pions. This approach maintains good agreement with the average properties of nuclear matter [35]. We will explore in Sec. IV whether it can address the issues raised by the $(p,p')$ polarization data.

## II. CONVENTIONAL MEDIUM EFFECTS

### A. DWIA calculations

The DWIA calculations reported here are made with the program DWBA86 [36].

This program is different from the one used to examine the natural-parity states in our previous work [3]. The exchange parts of the amplitude are calculated using finite range, which is important in general for the treatment of the spin-dependent parts of the effective interaction.

The transition form factors are calculated assuming that a single particle-hole configuration is dominant. For the $4^-$ states in $^{16}$O, this is $p_{3/2}^{-1}d_{5/2}$, and for the $6^-$ states in $^{28}$Si it is $d_{5/2}^{-1}f_{7/2}$. In each case the transition goes from an orbital that is filled in the simple shell model to one that is empty. The change of orbital angular momentum by one unit introduces the negative parity in both cases. While other configurations can be constructed that couple to the same value of spin and parity, they involve orbitals at much higher excitation. Those most likely to contribute, such as $p_{3/2}^{-1}g_{9/2}$ in the $6^-$ case, do not change the DWIA calculation since they are also stretched configurations with the same $L$-transfer. To find particle-hole configurations where $j_p+j_h>J$, orbitals at even higher excitation are required, and significant transition strength there is unlikely. Once the particle and hole wave functions for the single configuration are adjusted to reproduce the $(e,e')$ transverse form factor measurements, we consider the structure of the transition sufficiently well constrained that we can safely judge the quality of the other ingredients in the calculation.

The particle and hole wave functions are calculated as states in a Woods-Saxon well. The binding energies are chosen to represent the energy needed to separate a proton or a neutron, leaving behind the lowest state with the required spin and parity. For $^{28}$Si, these are the $5/2^+$ ground states of $^{27}$Al and $^{27}$Si. In the case of the $T=1$, $6^-$ state at 14.35 MeV in $^{28}$Si, the $f_{7/2}$ proton added to the $^{27}$Al ground state is unbound by 2.78 MeV, an energy that is greater than the top of the Coulomb barrier for $^{27}$Al. In this case the wave function is calculated using the techniques developed by Vincent and Fortune [37]. For the $^{16}$O case, the ground states of the nuclei with one less proton or neutron are not $3/2^-$. Instead, we use the state at 6.324 MeV in $^{15}$N and the state at 6.176 MeV in $^{15}$O. Again for the $d_{5/2}$ proton, two of the three $4^-$ transitions require positive proton binding energies (0.53 and 1.36 MeV).

The Woods-Saxon geometry parameters (radius and diffuseness), as well as the spectroscopic factor, are adjusted until a calculation of the transverse form factor [38] in $(e,e')$ inelastic scattering reproduces the measurements. For

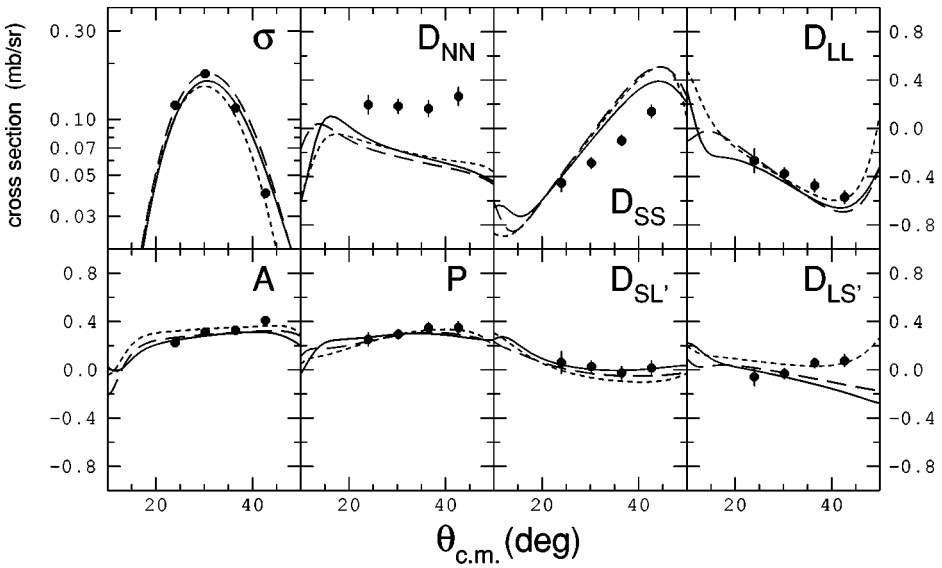


FIG. 1. Measurements of the cross section and polarization observables for the $6^-$, $T=1$ state at 14.35 MeV in $^{28}$Si [12,16]. The calculations represent the DBHF (solid), BHF (long dashed), and free (short dashed) effective interactions.

$^{16}$O we use the data of Hyde-Wright [39]; and for $^{28}$Si the data of Yen [40]. Because the transverse electron scattering form factor is mainly sensitive to the isovector part of the transition density, data is available only for three of the five transitions we consider. These include the $T=1$ states in $^{16}$O (18.98 MeV) and $^{28}$Si (14.35 MeV). In addition, the isospin mixing is such that there is also information available for the lower $4^-$ state in $^{16}$O (17.78 MeV) [39]. Thus we should expect quantitative agreement with the cross section only for these three cases. For the remaining two states, a form factor is chosen which is similar to that for the other states in the same nucleus. The spectroscopic factor will incorporate information from pion inelastic scattering, but reaction mechanism ambiguities prevent this from being a strong constraint. In these two cases, only the polarization observables will be useful in the evaluation of medium effects.

The distorted waves in the incident and exit channels are calculated using a folding model potential in which the central and spin-orbit terms in the effective interaction are averaged over the distribution of target nucleons. This distribution is taken from the charge density for each nucleus [41] by unfolding the contribution of the proton charge distribution. It is assumed for the two $N=Z$ nuclei considered here that the proton and neutron distributions are the same. This matter distribution is also used to determine the local density at which the effective *NN* interaction is evaluated. The folding model potential calculation is made with the distorted wave program LEA [42], and the local potential transferred to DWBA86.

The three $4^-$ states in $^{16}$O are isospin mixed. A three-state mixing model has been adjusted to reproduce the results of electron and pion scattering [43]. We will use those mixing ratios here. For the upper $T=0$ state at 19.80 MeV, we will use the same bound-state parameters and spectroscopic factor as the lower $T=0$ state with the changes from the isospin mixing model preserved.

For the $6^-$ states in $^{28}$Si, the energy separation is large enough that it is possible to consider them as unmixed, with the lower (11.58 MeV) being $T=0$ and the upper (14.35 MeV) being $T=1$ [43]. In the absence of electron scattering

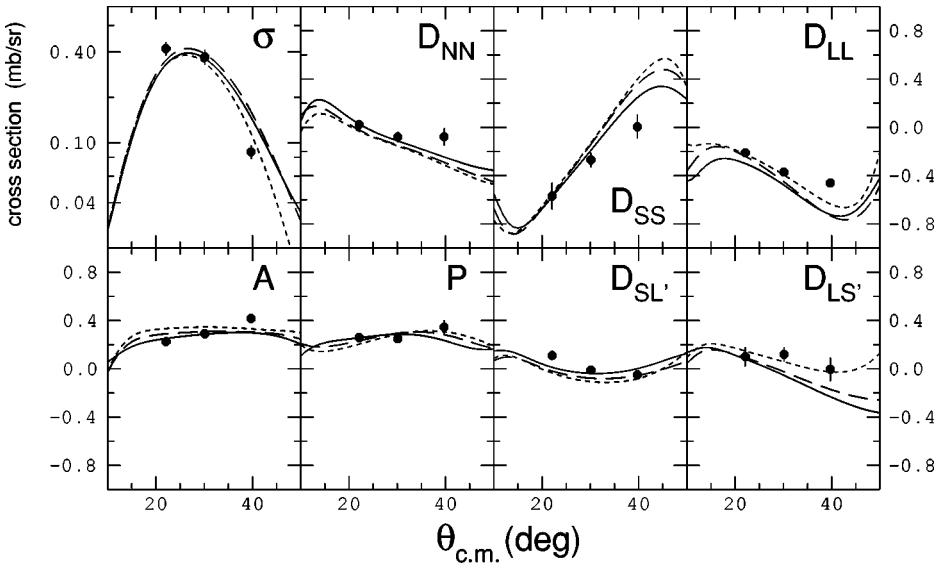


FIG. 2. Measurements of the cross section and polarization observables for the $4^-$, $T=1$ state at 18.98 MeV in $^{16}$O [13–15]. The calculations represent the DBHF (solid), BHF (long dashed), and free (short dashed) effective interactions.

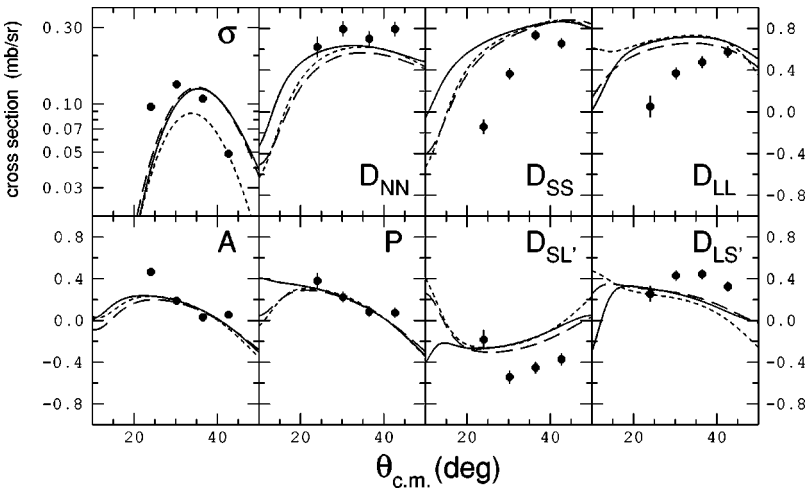


FIG. 3. Measurements of the cross section and polarization observables for the $6^-$, $T=0$ state at 11.58 MeV in $^{28}$Si [12,16]. The calculations represent the DBHF (solid), BHF (long dashed), and free (short dashed) effective interactions.

data for the $T=0$ transition, we will use the same bound state parameters as for the $T=1$ state and adjust the spectroscopic factor downward by 0.39 to be consistent with the findings of Olmer for pion scattering [44]. The question of whether some small isospin mixing would help us to understand the results for the $T=1$ state will be considered in the last part of this section.

### B. Comparison with data

Figures 1 and 2 show measurements and calculations for the two $T=1$ states, and Figs. 3–5 show the same for the $T=0$ states. In each case all observables, including the cross section, analyzing power, induced polarization, and five polarization transfer coefficients are shown. There are three calculations based on the effective interaction described in Ref. [3]. The short-dash curves make use of a free (density-independent) *NN* interaction. The long-dash curves are based on a *G*-matrix calculation which includes the Pauli blocking and binding energy medium effects from Brueckner theory only (BHF). The solid curves are also density-dependent, but include in addition the changes brought about through a consideration of the strong relativistic mean-field potentials in the Dirac-Brueckner approach to nuclear matter (DBHF).

The cross sections all show a roughly Gaussian distribution with momentum transfer and a peak location tied to the $L$ transfer. In the plane wave limit, not all of the polarization observables are independent [1,2]. In the absence of contributions from nuclear currents [11], the observables tend to follow the relationships $A=P$ and $D_{SL'}=-D_{LS'}$. The magnitudes of $A$, $P$, $D_{SL'}$, and $D_{LS'}$ are a measure of the interference between spin-orbit and tensor contributions to the reaction amplitude [1]. For the isovector transitions (Figs. 1 and 2), the spin-orbit part of the effective interaction is small, hence these four observables are all close to zero. This is not the case in the isoscalar channel (Figs. 3–5) where the spin-orbit amplitude is large and there are important exchange contributions to the tensor part of the interaction. In this case, these observables are larger.

The diagonal polarization transfer coefficients, $D_{NN}$, $D_{SS}$, and $D_{LL}$, are sensitive to the balance between spin-orbit and tensor components of the effective interaction. They will be discussed in more detail in the next subsection.

Except for the $T=0$ cross sections (Figs. 3–5), there is little difference among the three calculations. For the BHF case, medium modifications to the tensor parts of the effective *NN* interaction are expected to be small [45].

The real spin-orbit and tensor parts of the effective *NN* interaction arise mainly from specific terms in the OBE potential. For the isovector tensor, this comes from the balance between $\pi$- and $\rho$-meson exchange potentials. For the isos-

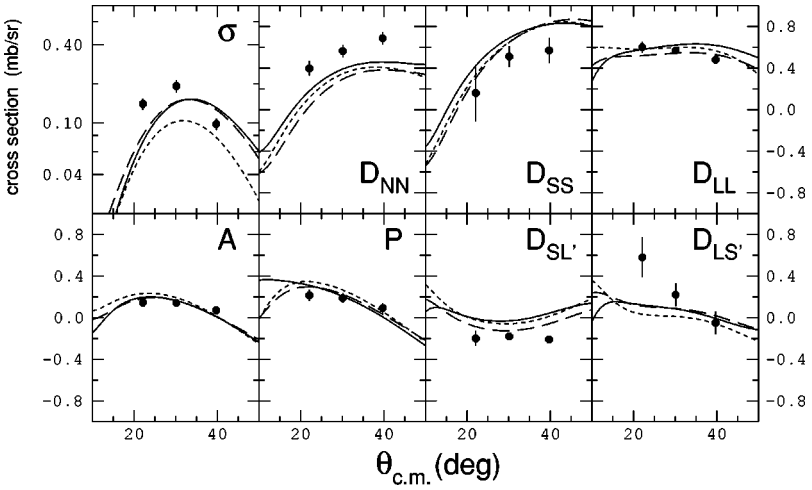


FIG. 4. Measurements of the cross section and polarization observables for the $4^-$, $T=0$ state at 17.78 MeV in $^{16}$O [13–15]. The calculations represent the DBHF (solid), BHF (long dashed), and free (short dashed) effective interactions.

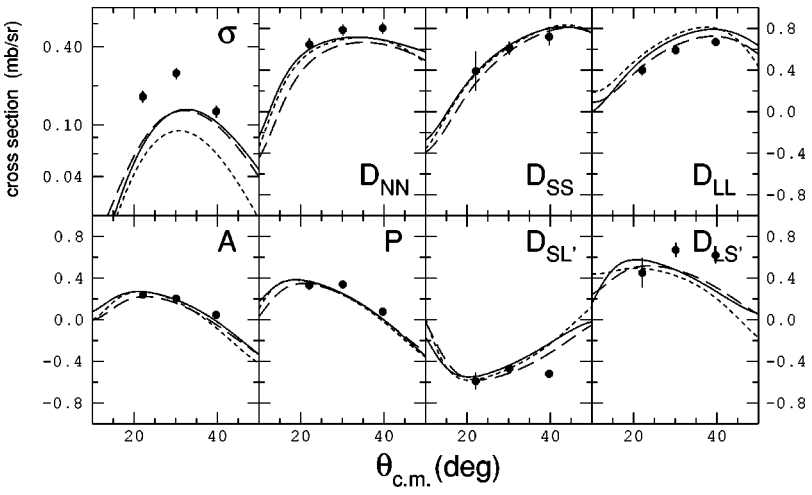


FIG. 5. Measurements of the cross section and polarization observables for the $4^-$, $T=0$ state at 19.81 MeV in $^{16}$O [13–15]. The calculations represent the DBHF (solid), BHF (long dashed), and free (short dashed) effective interactions.

calar spin-orbit, this is $\sigma$- and $\omega$-meson exchange, and for the isoscalar tensor $\omega$- and $\eta$-meson exchange [which nearly cancels to zero, leaving the isovector tensor as the main contribution to $(p,p')$ reactions through the exchange part of the DWIA calculation]. For the Dirac-Brueckner (DBHF) calculation, the effective nucleon mass also changes the potential terms in the scattering equation, but this has little effect on the OBE potentials for the $\pi$ and $\rho$ mesons. Thus little difference is seen among the three curves in Figs. 1–5 for the polarization observables, especially where the cross section is largest. Some of the difference may also be due to the different optical model wave functions associated with the BHF and DBHF effective interactions.

For the two $T=1$ transitions in Figs. 1 and 2, the constraint of reproducing the electron scattering form factor results in satisfactory agreement with the cross section, although the medium effects tend to push the large-angle values upward away from the data. This is in contrast to the case for natural-parity transitions [3] where DWIA calculations systematically overestimate the cross section by as much as 50%. The calculations also reproduce the angular distributions of $A$, $P$, $D_{SL'}$, and $D_{LS'}$. It is only for the diagonal $D_{ii}$ that we see substantial disagreements, with the calculations being too positive for $D_{SS}$ and too negative for $D_{NN}$. Between the two transitions, the calculations are almost identical, a reflection of the similarity in the spin structure for all stretched transitions. While the discrepancies with data are similar in kind, the size of the disagreement depends on the target, particularly for $D_{NN}$ where the data are more positive for $^{28}$Si than for $^{16}$O.

For the two nominally $T=0$ states in $^{16}$O (Figs. 4 and 5), the amount of $T=1$ amplitude included with the $T=0$ is of opposite sign but about the same size. There are electron scattering measurements to constrain the $4^-$ form factor for the state at 17.79 MeV in $^{16}$O (Fig. 4). For this case we get rough agreement with the size of the cross section. Rescaling the $T=0$ $^{28}$Si transition downward by almost a factor of three to agree with the pion scattering results also yields reasonable agreement with the magnitude of that cross section. For the state at 19.80 MeV in $^{16}$O, the measured cross section is larger than the calculated one, despite using pion scattering information as an independent normalization. This discrepancy is not understood. It must be noted that the cross section, which comes mostly from the spin-orbit part of the isoscalar effective interaction, is enhanced by the density dependence. This is important in achieving any agreement with the calculations, and confirms the large density dependence present in the isoscalar spin-orbit part of the DBHF calculation. In all three $T=0$ cases, the large increase in the cross section when the density dependence is included also pushes the cross section peak to larger scattering angles while the data suggest that the opposite effect is needed. This arises because the effects of the density dependence on the isoscalar spin-orbit term grow with momentum transfer, a trend which is not supported by these data or the analysis of Ref. [3].

Whatever problems exist with the DWIA calculations, they appear to be worse for silicon than oxygen. Whether this points to a dependence on increasing mass or spin transfer, or arises from a structural change in the transition, is not known.

### C. Combinations of observables

For stretched transitions, there is (within certain approximations) a one-to-one correspondence between combinations of the polarization transfer observables and the sizes of individual amplitudes in the effective interaction, in combination with the appropriate structure factor [1,2]. This is most clear for the KMT form of the *NN* interaction [17] given by

$$M=A+B\sigma_{1n}\sigma_{2n}+C(\sigma_{1n}+\sigma_{2n})+E\sigma_{1q}\sigma_{2q}+F\sigma_{1p}\sigma_{2p}, \tag{1}$$

where $\sigma$ is the Pauli spin operator for particle 1 or 2 acting along the direction $\hat{n}$ (normal to the scattering plane), $\hat{q}$ (along the direction of the momentum transfer), or $\hat{p}(=\hat{q}\times\hat{n})$. The magnitude of each of the spin-dependent amplitudes in Eq. (1) is related to a single combination of polarization transfer coefficients $D_i$ cast in the form of a polarized cross section as

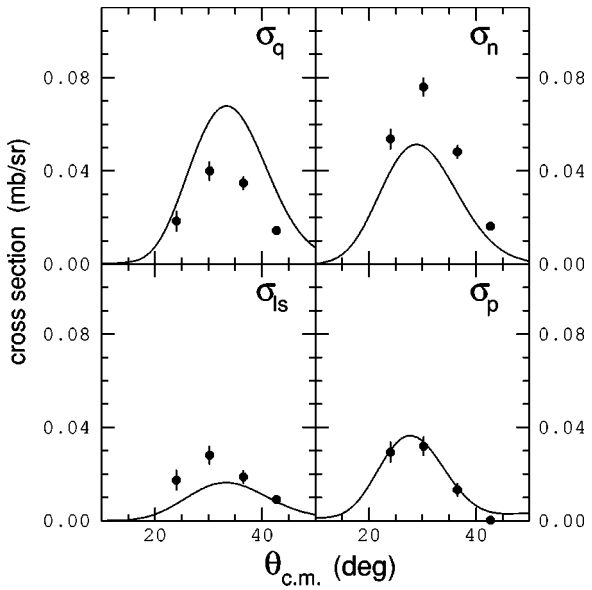


FIG. 6. Measurements of the polarized cross sections for the $6^-$, $T=1$ state at 14.35 MeV in $^{28}$Si [12,16]. The calculations represent the DBHF effective interaction.

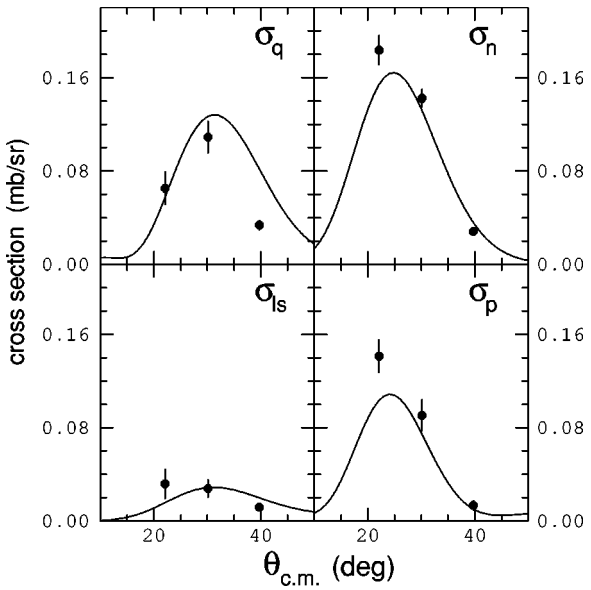


FIG. 7. Measurements of the polarized cross sections for the $4^-$, $T=1$ state at 18.98 MeV in $^{16}$O [13–15]. The calculations represent the DBHF effective interaction.

$$\sigma D_{ls}=C^2\chi_T^2, \quad \sigma D_q=E^2\chi_L^2,$$

$$\sigma D_n=B^2\chi_T^2, \quad \sigma D_p=F^2\chi_T^2, \tag{2}$$

where $\chi_L$ is the spin longitudinal form factor and $\chi_T$ is the transverse form factor. For stretched transitions, the formfactors are determined from the transverse electron scattering form factor and the relationship $\chi_L^2=2J\chi_T^2/(J+1)$. (All of the $D_i$ must be non-negative, a fact that limits the range over which the polarization transfer coefficients may vary.) The observable combinations $D_i$ are given by

$$D_{ls}=[1+D_{NN}+(D_{SS}+D_{LL})\cos\theta-(D_{LS'}-D_{SL'})\sin\theta]/4, \tag{3}$$

$$D_q=[1-D_{NN}+D_{SS}-D_{LL}]/4, \tag{4}$$

$$D_n=[1+D_{NN}-(D_{SS}+D_{LL})\cos\theta+(D_{LS'}-D_{SL'})\sin\theta]/4, \tag{5}$$

$$D_p=[1-D_{NN}-D_{SS}+D_{LL}]/4, \tag{6}$$

where $\theta$ is the center-of-mass scattering angle. The corresponding polarized cross sections are then defined as

$$\sigma_i=\sigma D_i\,. \tag{7}$$

A comparison with data is meaningful only for those three transitions where the transition form factor is constrained by electron scattering measurements.

From the combinations in Eqs. (3)–(6), it is possible to deduce some general features that are helpful in interpreting the differences shown in Figs. 1–5. If the scattering angle is small, and especially if $D_{LS'}$ and $D_{SL'}$ are also close to zero, we can set $\cos\theta\approx 1$ and $\sin\theta\approx 0$ and then invert Eqs. (3)–(6) to produce

$$D_{NN}=D_{ls}+D_n-D_q-D_p\,, \tag{8}$$

$$D_{SS}=D_{ls}-D_n+D_q-D_p\,, \tag{9}$$

$$D_{LL}=D_{ls}-D_n-D_q+D_p\,, \tag{10}$$

subject to the requirement

$$D_{ls}+D_n+D_q+D_p=1. \tag{11}$$

This makes it possible to quickly see how any change to one of the amplitudes in Eq. (2) might affect the diagonal polarization transfer coefficients, $D_{NN}$, $D_{SS}$, and $D_{LL}$. A change to the spin-orbit amplitude will move $D_{NN}$, $D_{SS}$, and $D_{LL}$ up and down together. If the spin orbit dominates, as it does for the isoscalar interaction, then these three polarization transfer coefficients are close to 1. Likewise, a change to any of the three tensor amplitudes will move one coefficient in one direction while sending the remaining two in the opposite direction. How the one-against-two pattern appears among the three coefficients then shows us which tensor amplitude needs to change.

In the plane wave limit, the vanishing of any spin-orbit contribution to the reaction means that $D_{NN}$ is purely negative [46]. This is a good approximation for the isovector part of the effective *NN* interaction [47]. If the spin-longitudinal part of the interaction becomes larger, then values of $D_{NN}$ become more negative. The measurements of $D_{NN}$ for the $T=1$ transitions are positive in the case of $^{28}$Si (Fig. 1) or near zero in the case of $^{16}$O (Fig. 2). Bringing $D_{NN}$ closer to zero requires a reduction of the pionlike, or spin-longitudinal, contribution to the effective interaction. But only a significant spin-orbit term can push $D_{NN}$ to positive values. These data show the need for a larger spin-orbit contribution to the isovector tensor interaction, as well as some changes among the tensor pieces.

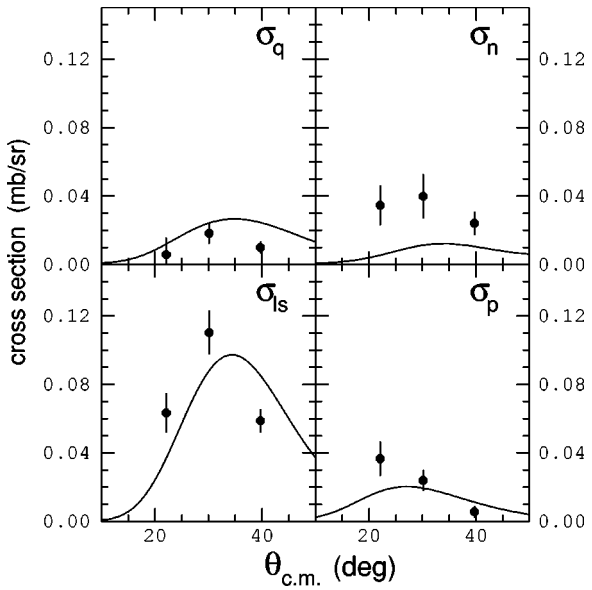


FIG. 8. Measurements of the polarized cross sections for the $4^-$, $T=0$ state at 17.78 MeV in $^{16}$O [13–15]. The calculations represent the DBHF effective interaction.

As was the case for the $T=1$ states, the differences between data and calculations for the $T=0$ transitions are larger for $^{28}$Si (Fig. 3) than for $^{16}$O (Figs. 4 and 5). The data for $D_{NN}$ are always more positive than the calculations. Measurements for $D_{SS}$, $D_{LL}$, and $D_{SL'}$ fall below their respective calculations while the opposite is observed for $A$ and $D_{LS'}$. The pattern in the diagonal polarization transfer coefficients indicates that $D_n$ should be larger relative to the dominant spin-orbit term in the isoscalar channel.

These conclusions are also evident upon inspection of the polarized cross sections of Eq. (7). In Figs. 6–8 the calculated polarized cross sections are compared with the data for the three transitions for which there is adequate form factor data. In all cases the calculations are DBHF, including all conventional medium effects. The $T=1$ transitions in $^{28}$Si and $^{16}$O are shown in Figs. 6 and 7. In both cases the spin-longitudinal cross section $\sigma_q$ is overestimated. Since the predictions for the cross section size are fairly close, this strength comes at the expense of the other polarized cross sections, in particular $\sigma_n$ and $\sigma_{ls}$. These differences are more extreme for $^{28}$Si than for $^{16}$O. In the case of $^{28}$Si, the necessity to increase the spin-orbit contribution in order to attain positive values of $D_{NN}$ is seen in Fig. 6 as an underestimate in $\sigma_{ls}$.

For the (mostly) $T=0$ transition at 17.78 MeV in $^{16}$O, the spin-orbit amplitude seems adequate but there is insufficient $\sigma_n$ tensor, as noted earlier. The increase of the density dependence with angle (or momentum transfer) for the spin-orbit interaction is apparent from $\sigma_{ls}$, where the peak is shifted to larger scattering angles.

In closing this subsection, we note again that this separation into four polarized cross sections helps us to identify which amplitudes in the effective *NN* interaction are most likely to be at fault when the calculations of the polarization transfer coefficients do not match the data.

### D. Isospin mixing for $^{28}$Si

One factor that may differ among nuclei is the degree of isospin mixing present in any particular stretched state. We recently suggested [48] that the large differences seen for the $T=1$ transition in $^{28}$Si might arise from the admixture of some $T=0$ strength. Tuning the amount of mixing based on the data available from Ref. [12] produced closer agreement, eliminating the overestimate for $\sigma_q$ shown in Fig. 6. Now, with a complete set of polarization transfer coefficients for this transition, it is possible to reevaluate this conclusion.

The isospin mixing of the $T=1$ transition in $^{28}$Si can be described, independent of its spectroscopic strength, by the angle $\eta$ in the expression $\cos\eta|p\rangle+\sin\eta|n\rangle$ where $|p\rangle$ and $|n\rangle$ are proton and neutron contributions to the transition. A pure $T=1$ transition lies at $\eta=135°$. For reference, this $T=1$ calculation is shown by dashed curves in Fig. 9 where the three observables were selected as the most sensitive to isospin mixing. A chi square minimization was made as a function of $\eta$, and the smallest value considering all the polarization data for this transition lies at $\eta=127.4°$. This calculation is represented by the solid curves in Fig. 9. The polarized cross section $\sigma_q$ improves, as does $D_{NN}$. But the combination $D_{SL'}-D_{LS'}$ becomes worse, indicating that the new contribution to the interference between spin-orbit and tensor interactions is inappropriate. (This information was not available for Ref. [48].) There is no value of $\eta$ that improves agreement for all observables, thus no reason to consider significant isospin mixing for this transition. Similar conclusions apply to the other transitions studied in this paper.

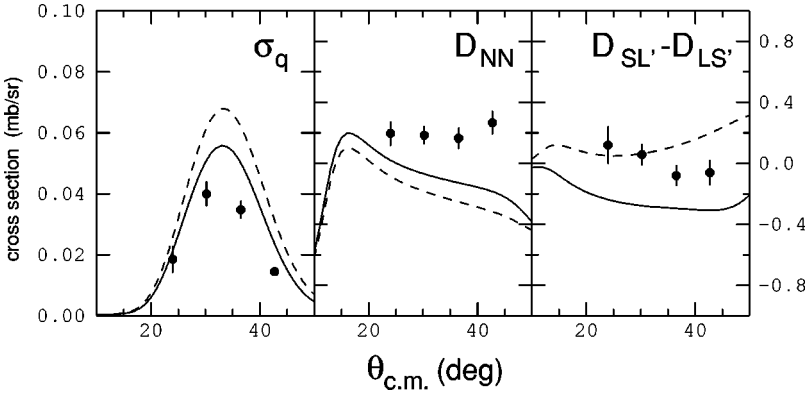


FIG. 9. Measurements of the $\sigma_q$ polarized cross section, $D_{NN}$, and the combination $D_{SL'}-D_{LS'}$ for the $6^-$, $T=1$ state at 14.35 MeV in $^{28}$Si [12,16]. The calculations represent isospin mixing with an angle of 135° (dashed, pure $T=1$) and 127.4° (solid).

### III. PREVIOUS WORK WITH $\rho$-MESON MASS SCALING

A number of attempts have been made to explain the differences between theory and experiment for the stretched $T=1$ transitions in terms of scaling of the $\rho$-meson mass in the nuclear medium. In all cases density-independent DWIA calculations have been used under the assumption that any change would correspond to some average density for the transition.

Stephenson and Tostevin [13] modeled the change in the effective *NN* interaction with an additional Yukawa term of short range that was chosen to resemble the change in the OBE potential with a reduced $\rho$-meson mass. They used a different Yukawa for the isovector spin-spin and tensor terms, and adjusted a complex coefficient for each until agreement was reached for the $^{16}$O polarization transfer observables. By comparing the real parts to a standard form for the $\rho$-meson potential [49], they found an average reduction of $\langle m^*/m\rangle = 0.938 \pm 0.016$. In another analysis, Baghaei *et al.* examined primarily measurements of $D_{NN}$ for the $3^+ \rightarrow 0^-$ transition in $^{10}$B and found $\langle m^*/m\rangle = 0.9$ [27]. In both cases, obtaining good agreement with the data required a careful adjustment of the imaginary parts of the interaction that arise from the density-dependent integral term in the scattering equation and thus have no simple connection to the OBE potential.

The appearance of even larger differences for $D_{NN}$ in $^{28}$Si prompted another analysis by Stephenson *et al.* [12]. In this case the amplitudes in the effective *NN* interaction were parametrized and adjusted to reproduce the data. The new amplitudes were then compared with OBE potential model calculations using a series of reduced $\rho$-meson masses. Values of $\langle m^*/m\rangle = 0.8$ seemed helpful for two of the four amplitudes considered, namely the ones associated with $\sigma_q$ and $\sigma_{ls}$.

To illustrate the effects of changing the $\rho$-meson mass in a density-independent calculation, we show in Fig. 10 the polarized cross sections for the $T=1$ state in $^{16}$O. The solid, long-dash, and short-dash curves represent interactions based on $\langle m^*/m\rangle = 1.0$, 0.9, and 0.8, respectively. For the three tensor components ($\sigma_q$, $\sigma_n$, and $\sigma_p$), the variations are roughly linear in $\Delta m = m - m^*$. The reduced tensor attraction is manifest in the reduction of $\sigma_q$ whose spin operator corresponds to pion exchange. Its counterpart $\sigma_p$, which can be associated with the pionlike tensor as it would appear for knock-on exchange contributions to the reaction, is also reduced. The changes to the spin-orbit seem to be highly nonlinear, and may contain the $\Delta m^3$ dependence discussed by Brown *et al.* [34]. The reduction needed to obtain better agreement for $\sigma_q$ and $\sigma_n$ lies between 10 and 20 %. Even though this represents the change at some average density for the transition, it is plausibly consistent with the expectation of a 20% reduction of the $\rho$-meson mass at full nuclear density.

We have repeated the calculation shown in Fig. 10 in a density-dependent environment in which the $\rho$-meson mass is assumed to scale down linearly with increasing density. The result is shown in Fig. 11, where the only density-dependence comes from the changing $\rho$-meson mass (no conventional *G*-matrix medium effects are included). Compared to Fig. 10, the effects are similar in kind but much smaller, and would suggest typical average densities of the order of 15–30 % for the stretched transition. At these densities, the effect of the expected change in $\rho$-meson mass is too small to be detectable in a comparison with these data. Results similar in size to those shown in Fig. 11 are obtained when the change to the $\rho$-meson mass is included along with the DBHF *G*-matrix calculation.

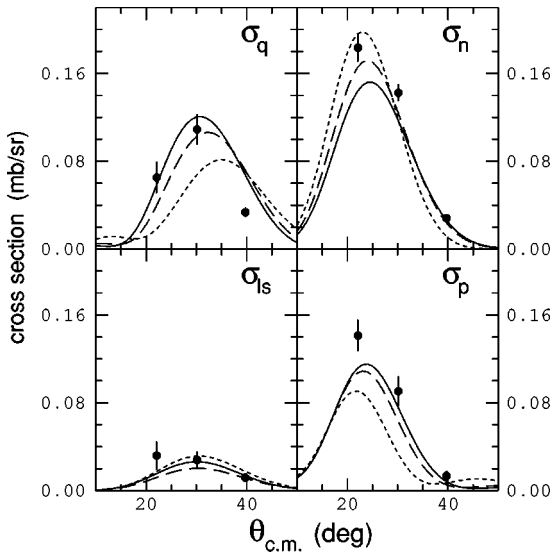


FIG. 10. Measurements of the polarized cross sections for the $4^-$, $T=1$ state at 18.98 MeV in $^{16}$O [13–15]. The calculations represent density independent interactions with the $\rho$-meson mass scaled as $\langle m^*/m\rangle = 1.0$ (solid), 0.9 (long dashed), and 0.8 (short dashed).

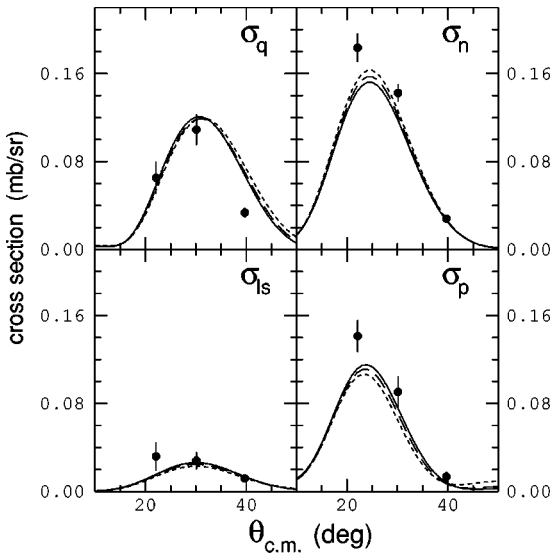


FIG. 11. Measurements of the polarized cross sections for the $4^-$, $T=1$ state at 18.98 MeV in $^{16}$O [13–15]. The calculations represent interactions with the only density dependence arising from a linear scaling of the $\rho$-meson mass with density where, at full nuclear matter density, $\langle m^*/m\rangle = 1.0$ (solid), 0.9 (long dashed), and 0.8 (short dashed).

In an analysis that considered a larger base of transitions, including both natural and unnatural parity, we considered variations of the meson masses in more detail [48,50]. Density-dependent mass modifications were used. The hope was to find some degree of freedom that would improve agreement across a large range of transitions and thus point toward physics missing from our model. It was found that a careful balance was needed between the $\sigma$- and $\omega$-meson masses in order to maintain the mean field for natural parity transitions. Beyond that, there was very little sensitivity to a scaling of the $\rho$-meson mass [50], thus confirming the conclusion reached here. Only if larger modifications were applied could some improvements be observed, but they were not systematic across all transitions being considered.

Simple scaling of the $\rho$-meson mass, like a modification to the isospin mixing, does not address the full range of differences observed for these $(p,p')$ transitions. This does not eliminate the possibility that a more comprehensive set of changes to the OBE meson properties based on additional physics considerations might contain the needed alterations to the spin dependence in the nuclear medium. One such model is evaluated in the next section.

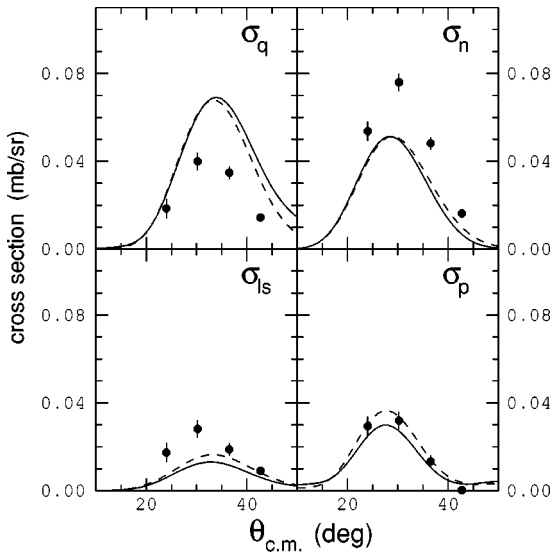


FIG. 12. Measurements of the polarized cross sections for the $6^-$, $T=1$ state at 14.35 MeV in $^{28}$Si [12,16]. The calculations represent the Rapp (solid) and DBHF (dashed) effective interactions.

## IV. A REALISTIC IN-MEDIUM MESON EXCHANGE MODEL

### A. Review of the model

In this section we consider an approach to the medium effects on the *NN* interaction that contains meson mass scaling and a more thorough treatment of the intermediate-range attraction typically described in terms of the $\sigma$ meson. The properties of this model have been captured in a OBE form [35] and we have incorporated it into our framework. First, we review the physical considerations underlying this new approach to nuclear matter.

One problem with meson mass scaling is the loss of nuclear matter saturation [34]. If the $\sigma$ and $\omega$ masses scale at the same rate, the increased attraction generated by the reduced-mass $\sigma$ will dominate over the corresponding increase in repulsion from the (reduced-mass) $\omega$, thus preventing saturation. This crucial observation is the starting point of the development of the model by Rapp *et al.* [35].

At a microscopic level, the fictitious $\sigma$ meson stands, in part, for a correlated pair of pions interacting in a relative *S* wave. The effect of the nuclear medium on the $\pi$-$\pi$ correlations has been investigated and observed to be very strong in the scalar-isoscalar channel [51]. However, this overly strong attraction (which is qualitatively similar to that of a reduced $\sigma$ mass in the OBE picture) can be moderated by the inclusion of $\pi$-$\pi$ contact interactions, which are repulsive in nature, while still allowing a realistic description of free pion-pion scattering [51]. These terms are required by chiral symmetry through the soft-pion theorem constraints on the scattering length [52].

It is shown in Ref. [35] that, when the microscopic, chirally-constrained $\pi$-$\pi$ interaction from Ref. [51] is used to describe the correlated *S*-wave $2\pi$ exchange, then the assumption of dropping meson masses, implemented within the DBHF framework, does indeed lead to nuclear matter saturation at the empirical density.

Starting with the OBE model of Ref. [3] (which reproduces accurately free *NN* scattering below 325 MeV), the zero-width $\sigma$ meson is replaced by the microscopic model for $2\pi$ exchange of Ref. [51]. This model contains chiral symmetry contact terms which considerably slow down the increase in attraction observed when the interaction is placed into the nuclear medium.

The $2\pi$ exchange model has been parametrized [35] in terms of two sharp scalar mesons with density-dependent masses and coupling constants. These density-dependent parameters are shown in Table I of Ref. [35]. The correlated $2\pi$ exchange thus described accounts for more than half the intermediate range attraction. The remaining attraction is then parametrized in terms of a scalar-isoscalar boson with approximately half the strength the usual $\sigma$ boson would have in a typical OBE potential. This combination for the intermediate range attraction reproduces the original free space potential from Ref. [3].

The Brown-Rho scaling scenario [19,20], together with the above mechanism to provide additional repulsion in the $2\pi$ sector, is then found to be consistent with stable nuclear matter. The scaling prescription is applied to nucleon and vector meson masses. Masses scale linearly to 85% of their free-space values at full nuclear matter density, which is consistent with QCD sum rules analyses [21–24].

### B. Comparison with the data

The predictions we obtain when using the Rapp prescription show similar effects for all states with the same isospin, so only a single example of each will be shown here. Figures 12 and 13 show calculations for the $T=1$ and $T=0$ stretched $6^-$ states in $^{28}$Si. The dashed curves use the DBHF model described earlier; the solid curves use the Rapp model.

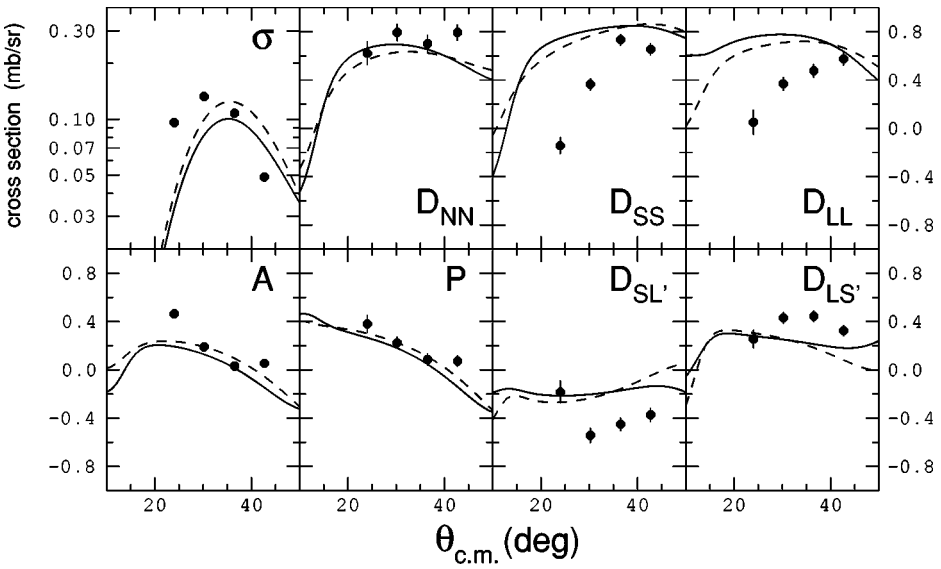


FIG. 13. Measurements of the cross section and polarization observables for the $6^-$, $T=0$ state at 11.58 MeV in $^{28}$Si [12,16]. The calculations represent the Rapp (solid) and DBHF (dashed) effective interactions.

Though some sensitivity to the change of model can be seen in some of the observables, particularly at the larger angles, a global look at the new calculation shows no overall significant improvement or deterioration in the quality of the predictions as compared to those from the DBHF model. This is true for both isospin channels.

The similarity between the DBHF and the Rapp predictions for these observables indicate that the two models must have a rather similar spin dependence. This can be further explored by comparing specific *G*-matrix elements from the two models. In Fig. 14(a), we show the $^3S_1$-$^3S_1$ matrix element at 200 MeV and nuclear matter density, as a function of the (half-off-shell) *NN* center-of-mass momentum, while Fig. 14(b) shows the $^3S_1$-$^3D_1$ transition under the same conditions. As before, the solid and the dashed curve are calculated within the Rapp and the DBHF model, respectively. We notice from Fig. 14(a) that the Rapp calculation for the $^3S_1$-$^3S_1$ case is considerably more repulsive than the DBHF curve, which is to be expected on the basis of the above discussion. The differences between the two curves in Fig. 14(a) most likely reflect differences in the central force originating from Rapp's handling of the intermediate range attraction as compared to DBHF. The matrix element shown in Fig. 14(a) also receives a contribution from the tensor force, which could in principle be partially responsible for the differences. But the small difference between the two curves in Fig. 14(b) indicates that the tensor force is very similar in the two models.

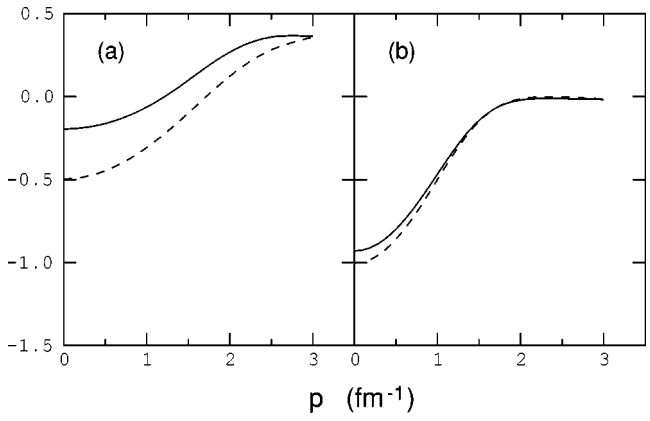


FIG. 14. Calculations of the real part of the half-off-shell matrix elements for the $^3S_1$-$^3S_1$ (a) and $^3S_1$-$^3D_1$ (b) transitions using the Rapp (solid) and DBHF (dashed) effective interactions.

While concluding that this prescription does not resolve the problems raised by these data, we must at the same time also notice that no deterioration in the overall quality of the predictions is observed, suggesting that we are looking at a case that is not sensitive to this level of scaling. Perhaps a process involving typically much higher densities is better suited to test a mass rescaling model such as the one we have applied here.

## V. SUMMARY AND CONCLUSIONS

We have examined the cross section, analyzing power, induced polarization, and polarization transfer coefficients for $(p,p')$ reactions to unnatural-parity, high-spin states in $^{16}$O and $^{28}$Si. We compared this data with DWIA calculations using an effective *NN* interaction derived within a microscopic treatment of nuclear medium effects. The model, which is based on a quantitative OBE potential and incorporates medium effects through a relativistic *G*-matrix approach, has been previously confronted with data for natural-parity, isoscalar transitions with satisfactory results [3].

The spin-flip nature of the states considered here restricts their sensitivity to the spin dependent parts of the effective interaction. The high-spin character emphasizes the single particle aspects of the nuclear structure, which are easily constrained by measurements of the electron scattering form factor.

Comparison with the data shows that the effects of conventional density dependence are essentially absent, except for the size of the spin-orbit interaction in the isoscalar channel. This particular density-dependent change appears for the $T=0$ cross section, where the agreement in size with the

DBHF calculation appears to confirm this effect. The shift of the angle of the maximum in the $T=0$ cross section would, however, suggest that the momentum transfer dependence of the changes to the isoscalar spin-orbit are incorrect. The DBHF calculation manifests some problems for stretched transitions, and the diagonal polarization transfer coefficients in particular. As illustrated by the decomposition into four polarized cross sections, these differences would suggest that the balance between spin-orbit and tensor components of the effective *NN* interaction still needs modification. For the $T=1$ transitions, the contrast between $^{16}$O and $^{28}$Si in the size of the discrepancies makes it difficult to assess the extent to which these differences can be addressed by systematic density-dependent changes to the effective interaction. Nevertheless, the overestimate of $\sigma_q$ remains in both cases, suggesting that there is still too much tensor attraction in the isovector channel. For the three $T=0$ transitions, the differences between data and theory are larger and more systematic. In these transitions, where the isoscalar spin-orbit component is the dominant contribution, there is a clear signature in the diagonal polarization transfer coefficients for an increase in the tensor interaction associated with $\sigma_n$. While a change in the isospin character of the transitions may alter the balance of spin-orbit and tensor components, a detailed investigation did not confirm the need for such a mechanism.

Because the observed discrepancies indicate the need to alter the balance between tensor and spin-orbit forces, a possible explanation was sought in terms of modifications of the underlying meson-exchange potential in the medium. A model which employs in-medium meson-exchange interactions while providing a satisfactory description of nuclear matter ground state properties has recently been proposed [35]. We applied this model but observed no significant changes in the quality of the predictions. This is consistent with our evaluation of past work, where it was observed that effects from linear scaling of the $\rho$ meson mass cannot be reliably detected through these data at the present level of experimental error and theoretical uncertainty.

Since open questions remain, we are prompted to continue looking for other mechanisms which can potentially alter the relative strength of the tensor and spin-orbit forces. A possibility can be identified in one of the sources of conventional density dependence, namely the Pauli projection operator, which has traditionally been handled through the angle-average approximation [5]. The quality of this approximation was explored about a decade ago and found satisfactory [53], even for inelastic scattering off-diagonal *G*-matrix elements. On the other hand, at the level of precision appropriate to present standards it may be reasonable to reexamine the validity of even well-established approximations, especially if they are likely to affect the spin-dependent terms.

## ACKNOWLEDGMENTS

One of the authors (F.S.) acknowledges financial support from the University of Idaho Physics Department and the University of Idaho Research Council. The IUCF authors acknowledge financial support from the National Science Foundation through Grant No. NSF-PHY-9602872.

[1] J. M. Moss, Phys. Rev. C **26**, 727 (1982).
[2] E. Bleszynski, M. Bleszynski, and C. A. Whitten, Jr., Phys. Rev. C **26**, 2063 (1982).
[3] F. Sammarruca, E. J. Stephenson, and K. Jiang, Phys. Rev. C **60**, 064610 (1999).
[4] V. G. J. Stoks *et al.*, Phys. Rev. C **48**, 792 (1993).
[5] M. I. Haftel and F. Tabakin, Nucl. Phys. **A158**, 1 (1970).
[6] M. R. Anastasio, L. S. Celenza, W. S. Pong, and C. M. Shakin, Phys. Rep. **100**, 327 (1983).
[7] R. Brockmann and R. Machleidt, Phys. Lett. **149B**, 283 (1984); Phys. Rev. C **42**, 1965 (1990).
[8] C. J. Horowitz and B. D. Serot, Phys. Lett. **137B**, 287 (1984); Nucl. Phys. **A464**, 613 (1987).
[9] B. ter Haar and R. Malfliet, Phys. Rep. **149**, 207 (1987).
[10] Jian Liu, E. J. Stephenson, A. D. Bacher, S. M. Bowyer, S. Chang, C. Olmer, S. P. Wells, S. W. Wissink, and J. Lisantti, Phys. Rev. C **53**, 1711 (1996).
[11] W. G. Love and J. R. Comfort, Phys. Rev. C **29**, 2135 (1984).
[12] E. J. Stephenson, J. Liu, A. D. Bacher, S. M. Bowyer, S. Chang, C. Olmer, S. P. Wells, and S. W. Wissink, Phys. Rev. Lett. **78**, 1636 (1997).
[13] E. J. Stephenson and J. A. Tostevin, in *Spin and Isospin in Nuclear Reactions*, edited by S. W. Wissink *et al.* (Plenum, New York, 1992), p. 281.
[14] C. Olmer, in *Antinucleon- and Nucleon-Nucleus Interactions*, edited by G. E. Walker *et al.* (Plenum, New York, 1985), p. 261.
[15] S. W. Wissink, in *Spin and Isospin in Nuclear Interactions*, edited by S. W. Wissink *et al.* (Plenum, New York, 1992), p. 253.
[16] Kehan Jiang, Ph.D. thesis, Indiana University, 1999.
[17] A. K. Kerman, H. MaManus, and R. M. Thaler, Ann. Phys. (N.Y.) **8**, 551 (1959).
[18] J. Bystricky, F. Lehar, and P. Winternitz, J. Phys. (Paris) **39**, 1 (1978).
[19] G. E. Brown and Mannque Rho, Phys. Lett. B **237**, 3 (1990); Phys. Rev. Lett. **66**, 2720 (1991); Phys. Rep. **269**, 334 (1996).
[20] G. E. Brown, M. Buballa, Zi Bang Li, and J. Wambach, Nucl. Phys. **A593**, 295 (1995).
[21] T. Hatsuda and S. Huong Lee, Phys. Rev. C **43**, 213 (1991).
[22] M. Asakawa and C. M. Ko, Phys. Rev. C **48**, R526 (1993).
[23] T. Hatsuda and T. Kunihiro, Phys. Rep. **247**, 221 (1994).
[24] Xuemin Jin and Derek B. Leinweber, Phys. Rev. C **52**, 3344 (1995).
[25] G. E. Brown, A. Sethi, and N. M. Hintz, Phys. Rev. C **44**, 2653 (1991).
[26] N. M. Hintz, A. M. Lallena, and A. Sethi, Phys. Rev. C **45**, 1098 (1992).
[27] H. Baghaei *et al.*, Phys. Rev. Lett. **69**, 2054 (1992).
[28] G. Q. Li, C. M. Ko, and G. E. Brown, Phys. Rev. Lett. **75**,

4007 (1995); Nucl. Phys. **A606**, 568 (1996).
[29] G. Q. Li, C. M. Ko, G. E. Brown, and H. Sorge, Nucl. Phys. **A611**, 539 (1996).
[30] G. J. Lolos *et al.*, Phys. Rev. Lett. **80**, 241 (1998).
[31] Ping Wang, Zhiwei Chong, Ru-Keng Su, and P. K. N. Yu, Phys. Rev. C **59**, 928 (1999).
[32] R. Rapp, G. Chanfray, and J. Wambach, Nucl. Phys. **A617**, 472 (1997).
[33] W. Cassing, E. L. Bratkovskaya, R. Rapp, and J. Wambach, Phys. Rev. C **57**, 916 (1998).
[34] G. E. Brown, H. Müther, and M. Prakash, Nucl. Phys. **A506**, 565 (1990).
[35] R. Rapp, R. Machleidt, J. W. Durso, and G. E. Brown, Phys. Rev. Lett. **82**, 1827 (1999).
[36] M. A. Schaeffer and J. Raynal, program DW81, as modified by S. M. Austin, W. G. Love, J. R. Comfort, and C. Olmer (private communication).
[37] C. M. Vincent and H. T. Fortune, Phys. Rev. C **2**, 762 (1972).
[38] B. L. Clausen, R. J. Peterson, and R. A. Lindgren, Phys. Rev. C **38**, 589 (1988).
[39] C. E. Hyde-Wright *et al.*, Phys. Rev. C **35**, 880 (1987).
[40] S. Yen *et al.*, Phys. Lett. B **289**, 22 (1992).
[41] H. deVries, C. W. de Jager, and C. de Vries, At. Data Nucl. Data Tables **36**, 495 (1987).
[42] J. J. Kelly, program LEA (private communication).
[43] J. A. Carr, F. Petrovich, D. Halderson, D. B. Holtkamp, and W. B. Cottingame, Phys. Rev. C **27**, 1636 (1983).
[44] C. Olmer *et al.*, Phys. Rev. Lett. **43**, 612 (1979).
[45] G. E. Brown, *Unified Theory of Nuclear Models and Forces* (North-Holland, Amsterdam, 1967), p. 184.
[46] W. G. Love, Amir Klein, M. A. Franey, and K. Nakayama, Can. J. Phys. **65**, 536 (1987).
[47] W. G. Love and M. A. Franey, Phys. Rev. C **24**, 1073 (1981).
[48] E. J. Stephenson and F. Sammarruca, in *New Facet of Spin Giant Resonances in Nuclei*, edited by H. Sakai *et al.* (World Scientific, Singapore, 1998), p. 369.
[49] J. Speth, V. Klempt, J. Wambach, and G. E. Brown, Nucl. Phys. **A343**, 382 (1980).
[50] E. J. Stephenson and F. Sammarruca, in *Intersections Between Particle and Nuclear Physics*, Proceedings of the Sixth Conference, edited by T. W. Donnelly, AIP Conf. Proc. No. 412 (AIP, New York, 1997), p. 708.
[51] R. Rapp, J. W. Durso, and J. Wambach, Nucl. Phys. **A596**, 436 (1996); **A615**, 501 (1997).
[52] S. Weinberg, Phys. Rev. Lett. **17**, 616 (1966); Phys. Rev. **166**, 1568 (1968).
[53] T. Cheon and E. F. Redish, Phys. Rev. C **39**, 331 (1989).